

Electronic Supporting Information (ESI)

Isothermal and Non-isothermal Cold Crystallization of Tetrabenzofluorene (TBF) Molecules

A. A. Boopathi^{ab}, Srinivasan Sampath^{c*} and T. Narasimhaswamy^{ab*}

^aPolymer Science & Technology Division, Council of Scientific and Industrial Research (CSIR)-Central Leather Research Institute (CLRI), Adyar, Chennai - 600020, India

^bAcademy of Scientific and Innovative Research (AcSIR), Ghaziabad - 201002, India

^cDepartment of Materials Science, School of Technology, Central University of Tamil Nadu, Thiruvarur - 610101, India

*tnswamy99@hotmail.com

*sampathsrinivasan@yahoo.com, srinivasansampath@cutn.ac.in.

[**] This research work was financially supported by DST-INSPIRE Faculty Award (IFA13-CH130). S.S and A.A.B acknowledge DST for the fellowship. We thank Dr. N. Somanathan, Dr. S. N. Jaisankar and Dr. Debasis Samanth for the fruitful discussion. We thank Chemical Physics, Bio-physics, Chemical and Organic laboratories in CSIR-CLRI and CATTERS in CSIR-CLRI, IIT-Madras and Madras University for sample analysis. We thank Dr. E. Bhoje Gowd, NIIST-Trivandrum for variable temperature PXRD analysis.

Experimental Details

Supplementary Information

Table of Contents

Experimental section

Section A. NMR studies of TBFC8- TBFC18	S3
Section B. Thermogravimetric Analysis (TGA) spectra of TBFC8 - TBFC18	S11
Section C. Differential Scanning Calorimetric (DSC) spectra and Hot-stage Polarising Microscopy (HOPM) images of TBFC8 - TBFC18	S12
Section D. Kissinger activation energy plot of TBFC10 - TBFC18	S19
Section E. Relative crystallinity versus temperature plot of TBFC10 & TBFC12	S21
Section F. Ozawa-Flynn-Wall analysis activation energy plot of TBFC10 - TBFC18	S21
Section G. Isothermal crystallization with five different temperatures range	S24
Section H. PXRD 2θ peaks intensity, FWHM (deg) and crystal size values are listed in table	S25
Section I. 2θ and h, k, l values of TBFC12 from single crystal PXRD	S29
Section J. References	S29

Experimental Section

Section A: NMR studies of TBFC8 to TBFC18

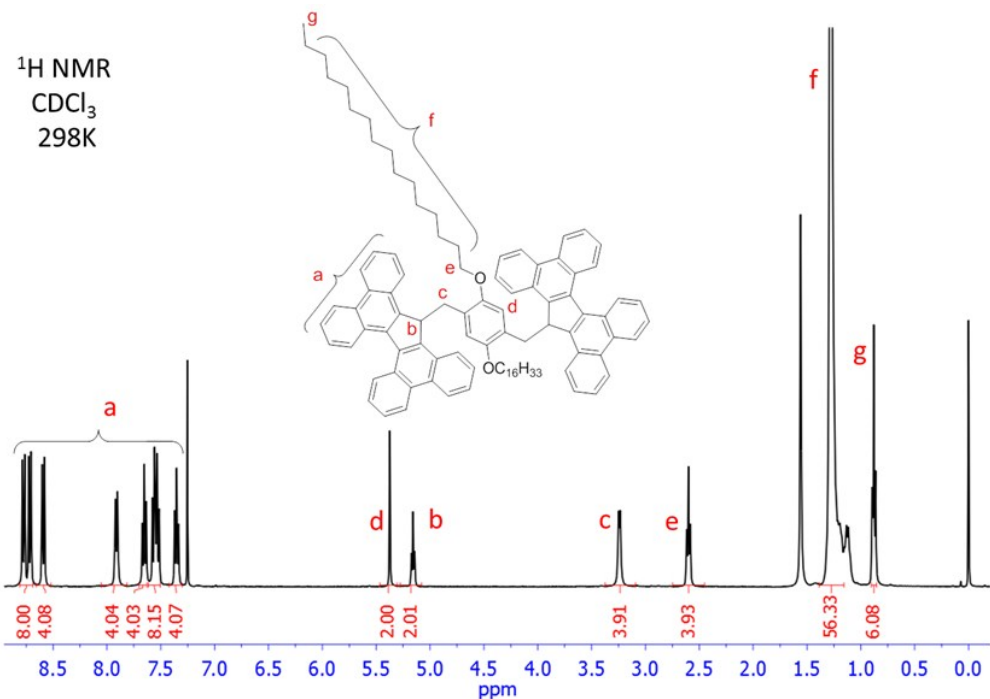


Figure S1. ¹H NMR spectrum of TBFC8 in CDCl₃ at 298 K

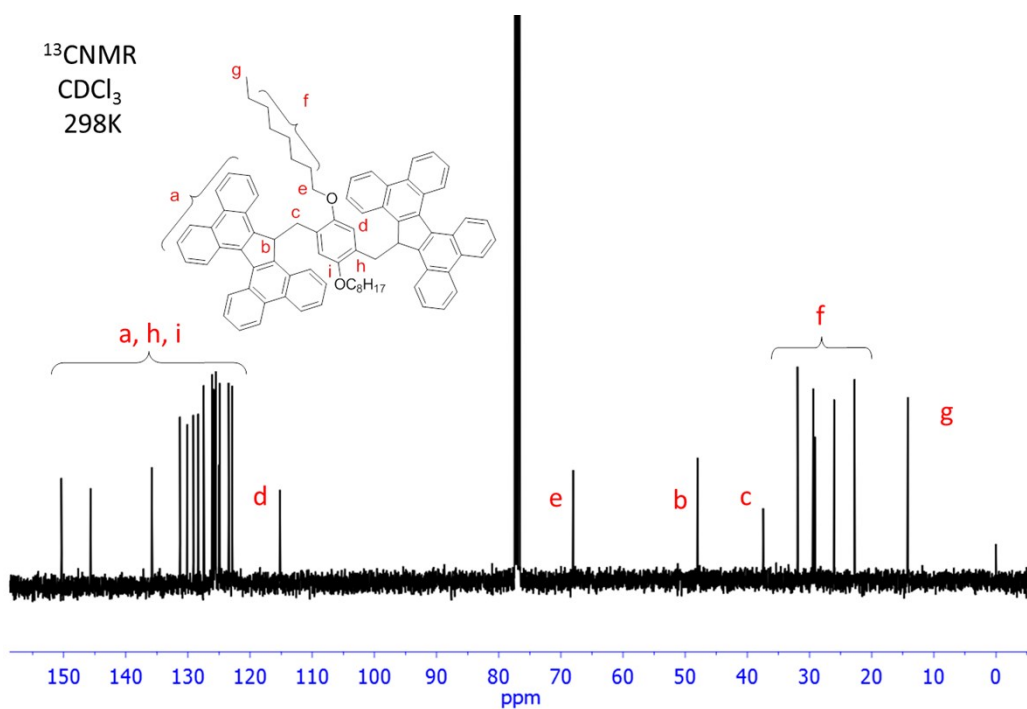


Figure S2. ^{13}C NMR spectrum of TBFC8 in CDCl_3 at 298 K

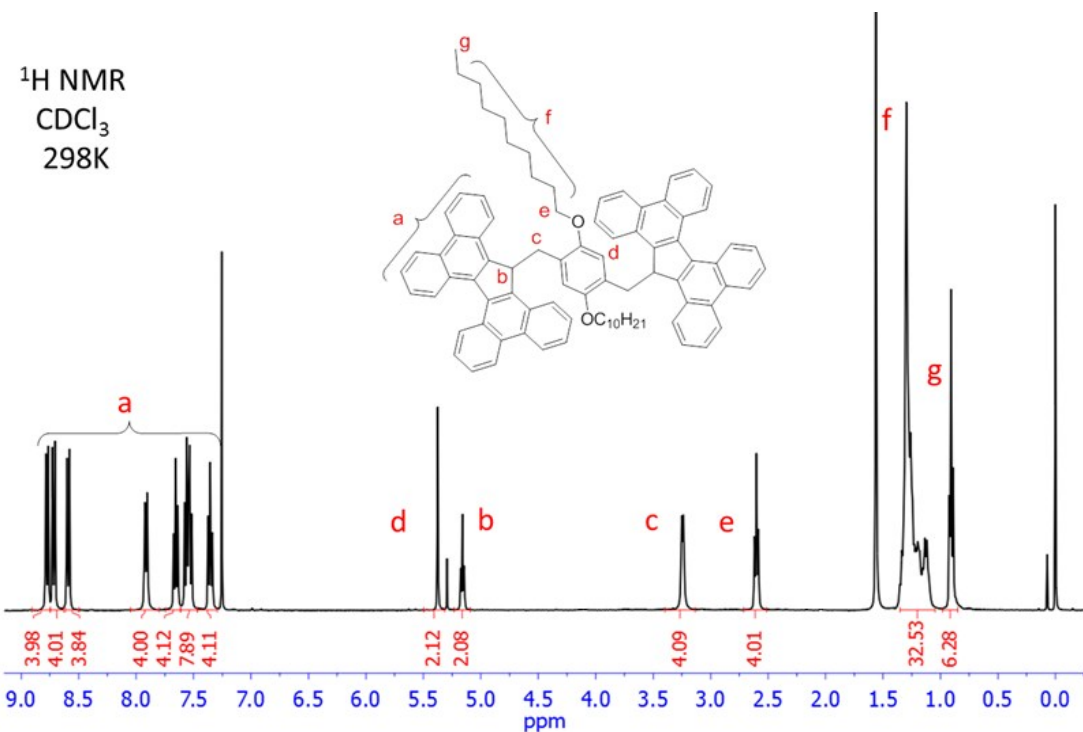


Figure S3. ^1H NMR spectrum of TBFC10 in CDCl_3 at 298 K

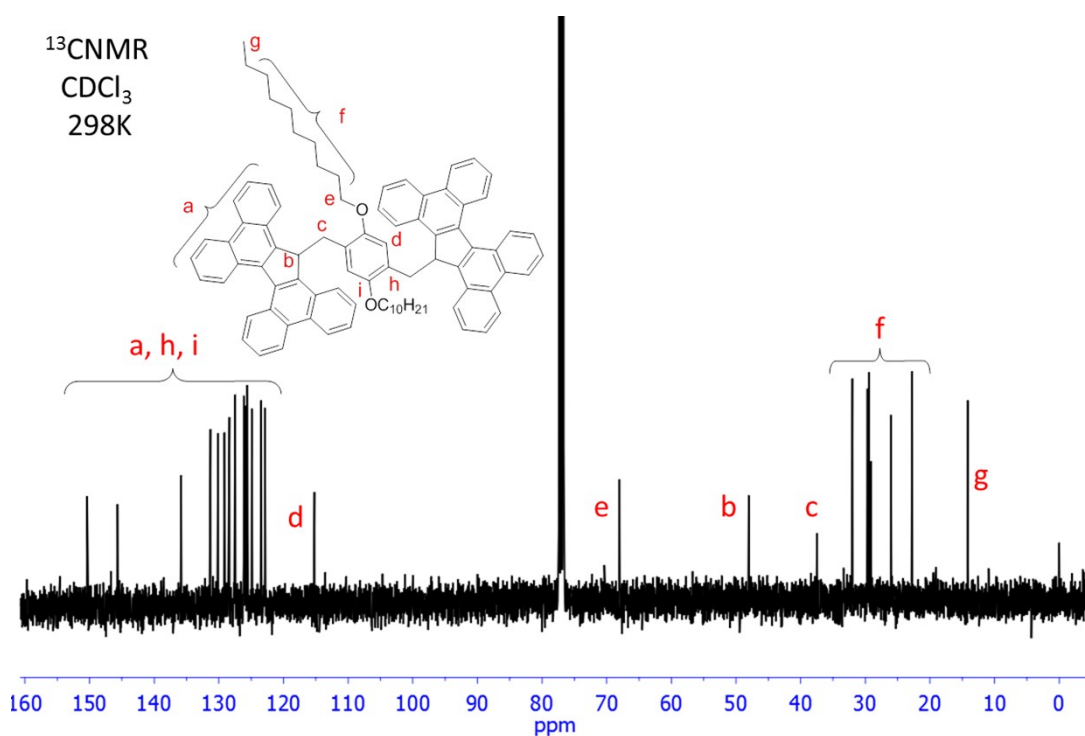


Figure S4. ^{13}C NMR spectrum of TBFC10 in CDCl_3 at 298 K

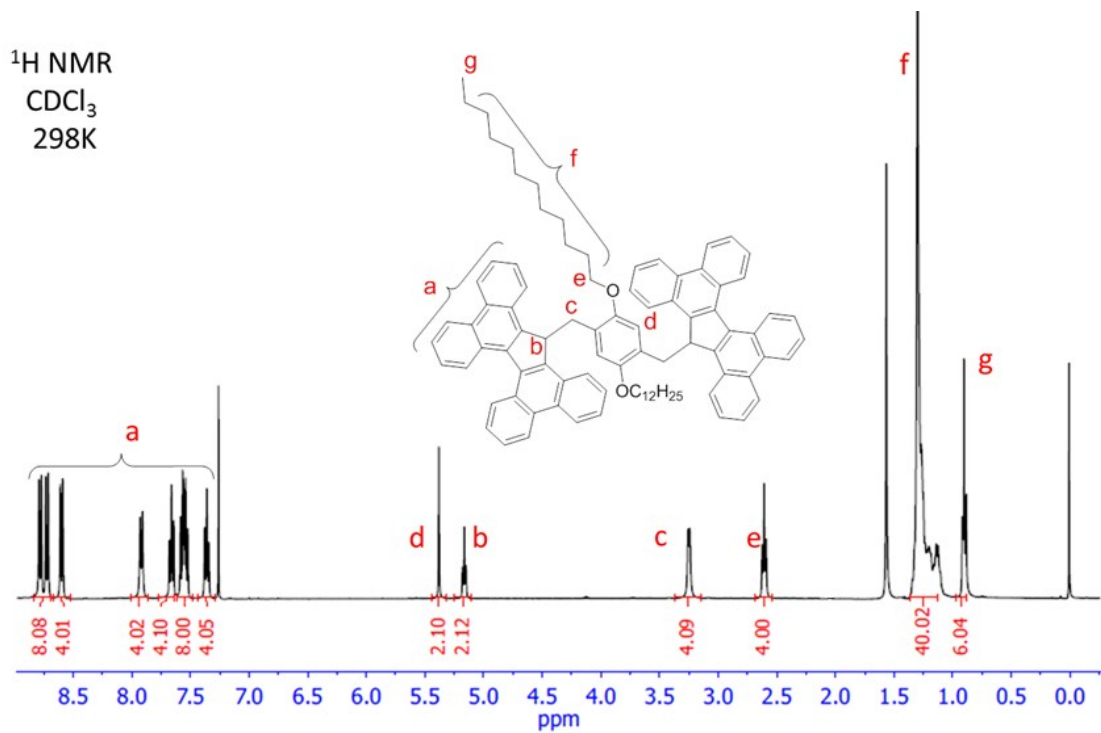


Figure S5. ¹H NMR spectrum of TBFC12 in CDCl_3 at 298 K

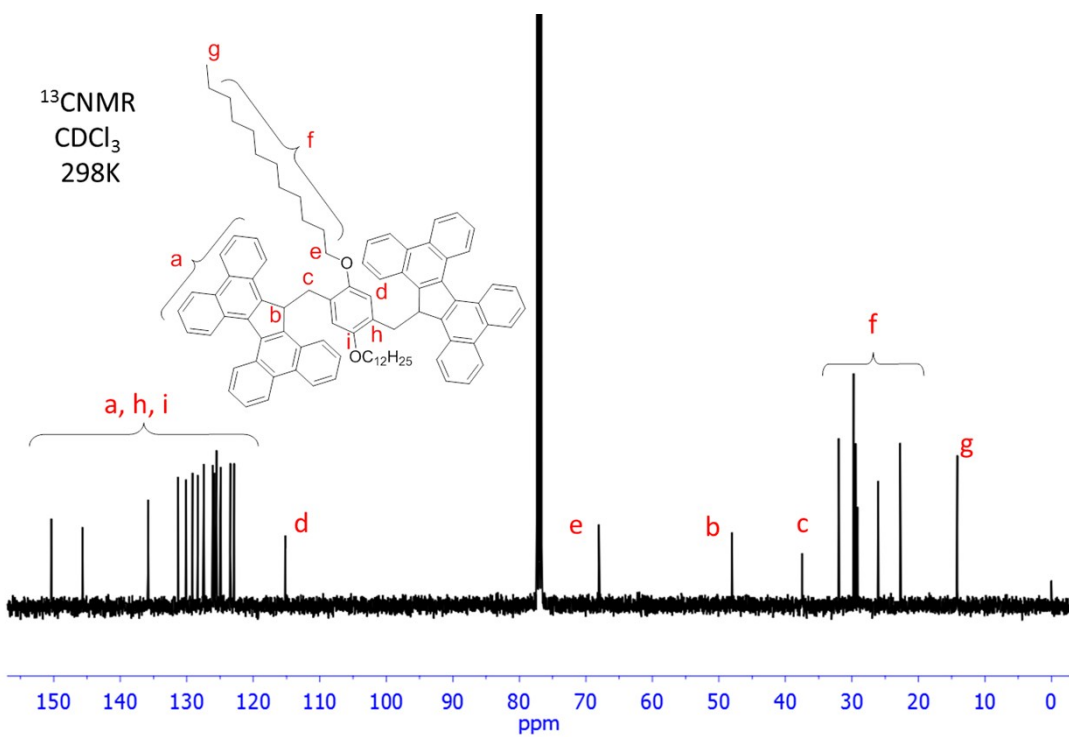


Figure S6. ¹³C NMR spectrum of TBFC12 in CDCl_3 at 298 K

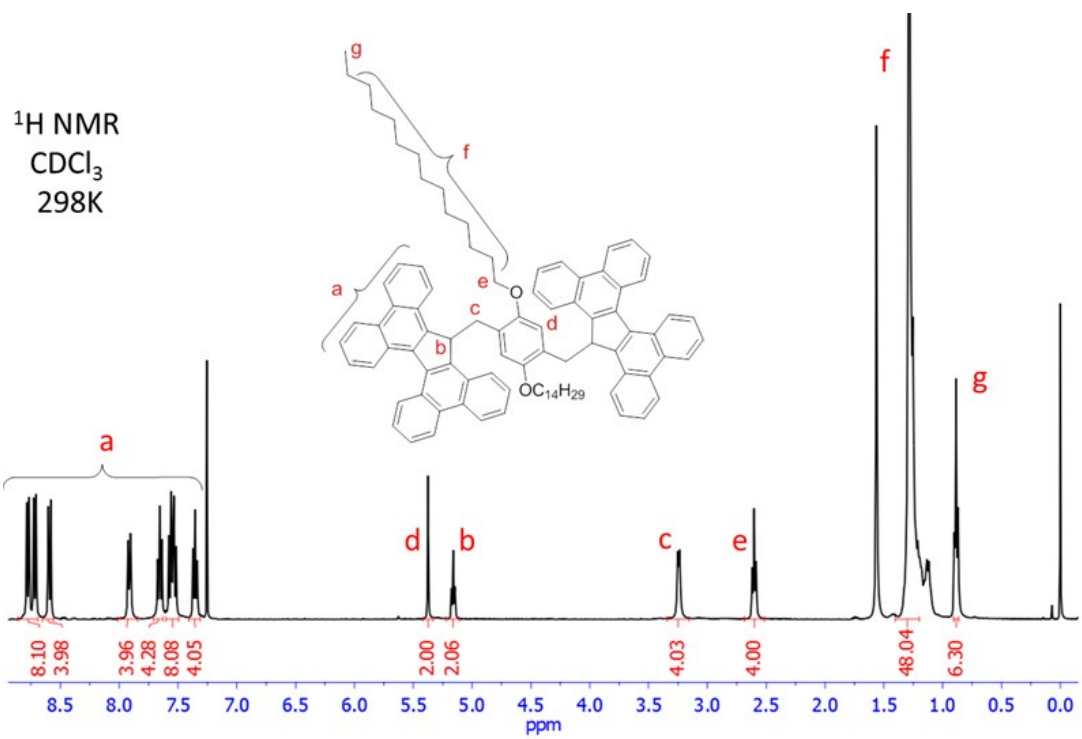


Figure S7. ¹H NMR spectrum of TBFC14 in CDCl_3 at 298 K

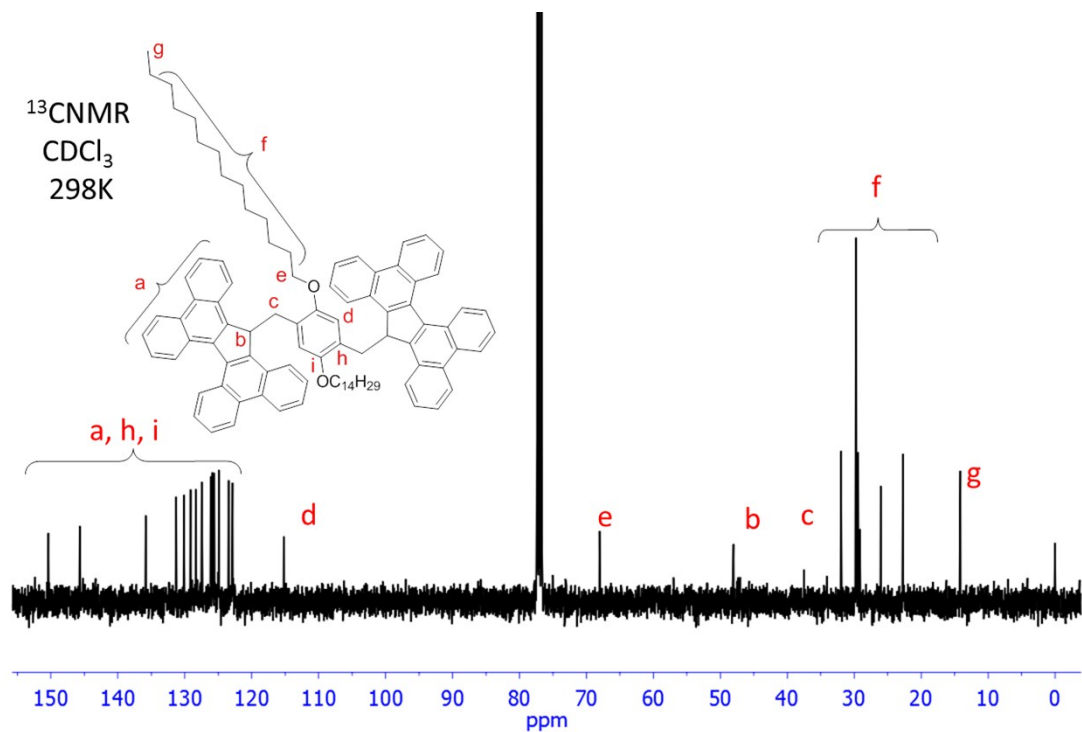


Figure S8. ¹³C NMR spectrum of TBFC14 in CDCl_3 at 298 K

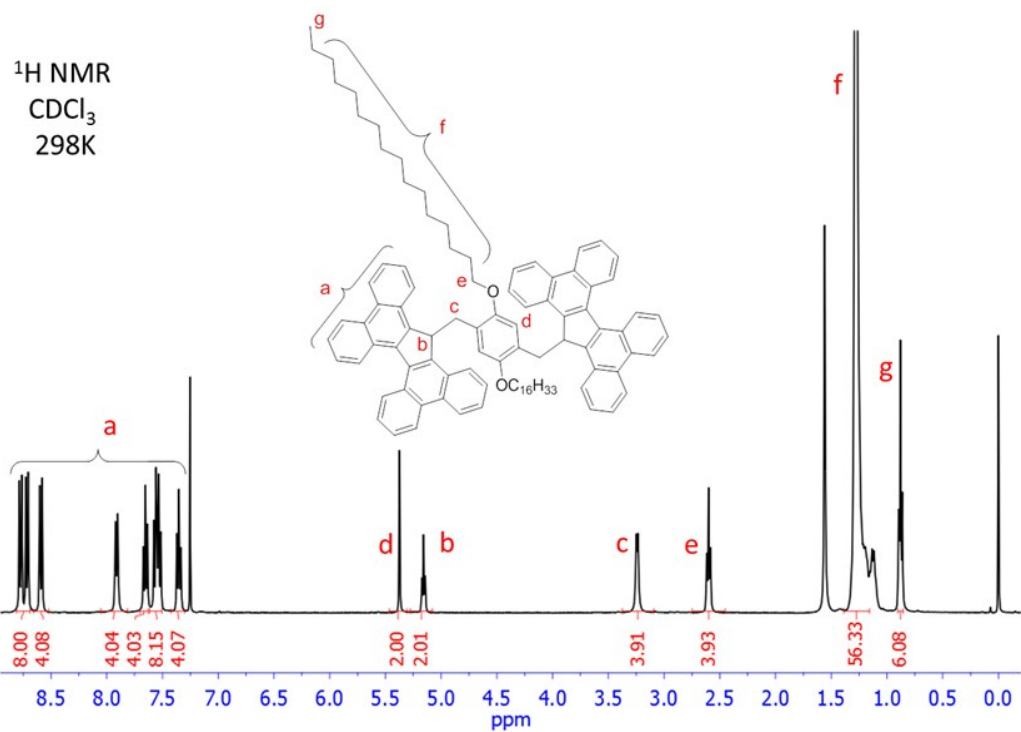


Figure S9. ¹H NMR spectrum of TBFC16 in CDCl_3 at 298 K

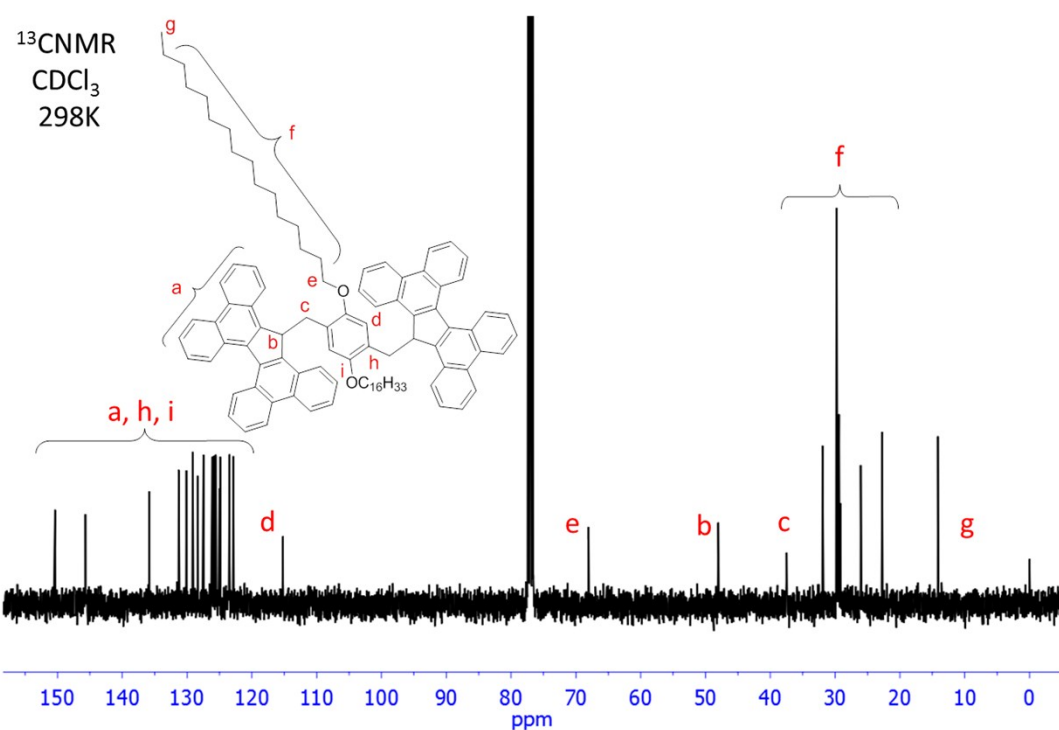


Figure S10. ¹³C NMR spectrum of TBFC16 in CDCl_3 at 298 K

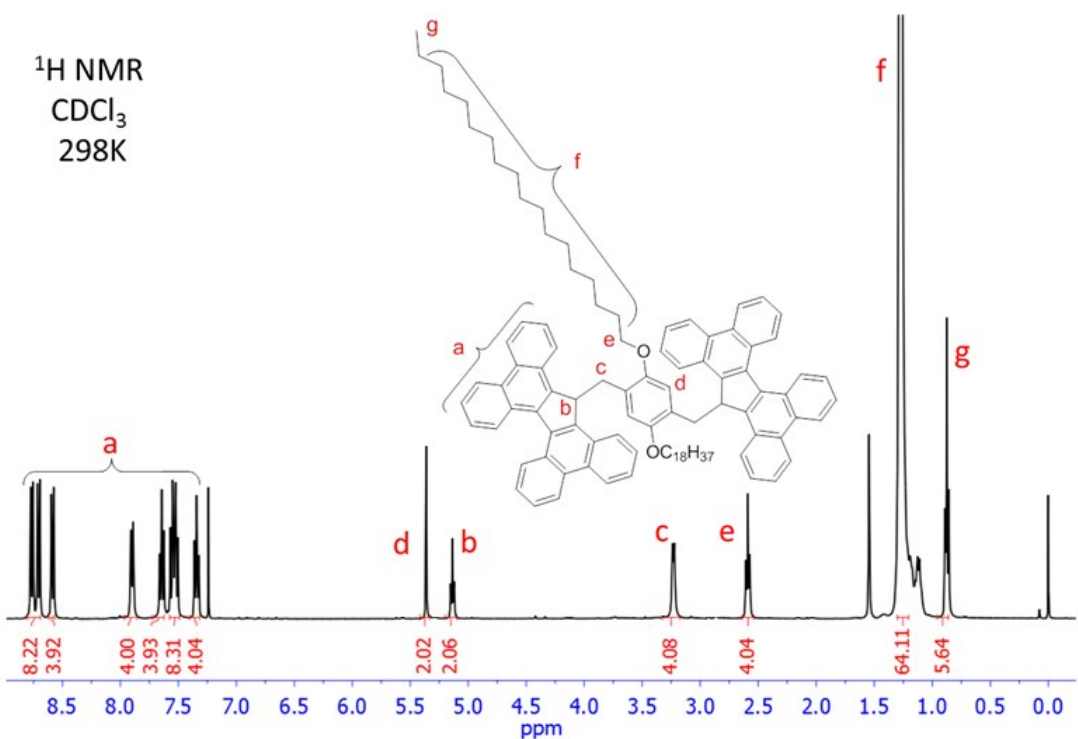


Figure S11. ¹H NMR spectrum of TBFC18 in CDCl_3 at 298 K

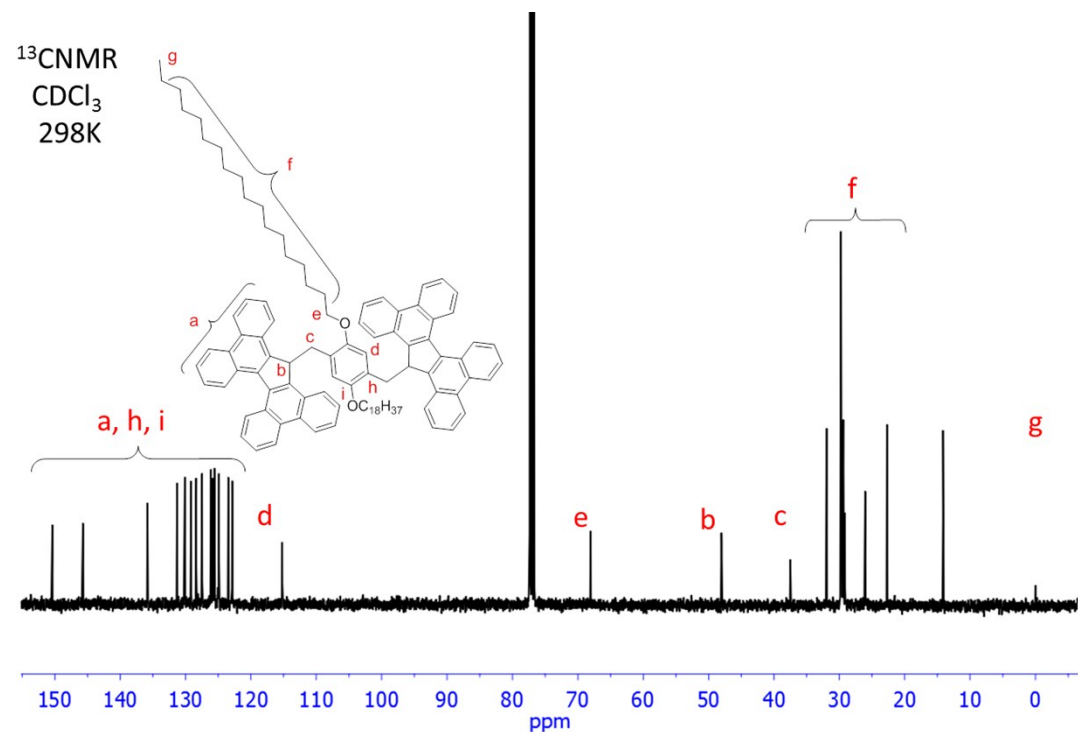


Figure S12. ¹³C NMR spectrum of TBFC18 in CDCl_3 at 298 K

The molecule (TBFC8) 1,4-bis(17H-tetrabenzo[a,c,g,i]fluorenemethyl)-2,5-bis(octyloxy)benzene: ^1H NMR (400 MHz, CDCl_3) δ 8.77 (d, $J = 8.2$ Hz, 4H), 8.71 (d, $J = 8.3$ Hz, 4H), 8.59 (d, $J = 8.1$ Hz, 4H), 7.91 (d, $J = 8.0$ Hz, 4H), 7.65-7.72 (m, 4H), 7.54-7.59 (m, 8H), 7.35 (t, $J = 7.4$ Hz, 2H), 5.37 (s, 2H), 5.15 (t, $J = 6.1$ Hz, 2H), 3.27 (t, $J = 18.0$ Hz, 4H), 2.59 (t, $J = 6.8$ Hz, 4H), 1.45 – 1.02 (m, 24H), 0.93 (t, $J = 6.9$ Hz, 6H). ^{13}C NMR (101 MHz, CDCl_3) δ 150.37, 145.68, 135.84, 131.30, 130.11, 129.14, 128.36, 127.46, 126.12, 125.87, 125.59, 125.54, 125.01, 124.90, 123.45, 122.87, 115.21, 77.34, 77.02, 76.70, 68.04, 48.03, 37.46, 31.93, 29.43, 29.39, 29.14, 26.04, 22.76, 14.19. MALDI-TOF MS: [M+Na]⁺ calculated for $\text{C}_{82}\text{H}_{74}\text{O}_2\text{Na}$: 1114.4535; found, 1114.4523. m.p.: 206.4 °C.

The molecule (TBFC10) 1,4-bis(17H-tetrabenzo[a,c,g,i]fluorenemethyl)-2,5-bis(decyloxy)benzene: ^1H NMR (400 MHz, CDCl_3) δ 8.78 (d, $J = 8.2$ Hz, 4H), 8.72 (d, $J = 8.3$ Hz, 4H), 8.59 (d, $J = 8.1$ Hz, 4H), 7.91 (d, $J = 8.0$ Hz, 4H), 7.65-7.72 (m, 4H), 7.55-7.60 (m, 8H), 7.35 (t, $J = 7.4$ Hz, 2H), 5.37 (s, 2H), 5.16 (t, $J = 6.1$ Hz, 2H), 3.24 (d, $J = 5.8$ Hz, 4H), 2.60 (t, $J = 6.8$ Hz, 4H), 1.12-1.40 (m, 32H), 0.91 (t, $J = 6.8$ Hz, 6H). ^{13}C NMR (101 MHz, CDCl_3) δ 150.37, 145.68, 135.84, 131.30, 130.11, 129.14, 128.36, 127.47, 126.12, 125.87, 125.59, 125.54, 125.01, 124.90, 123.45, 122.87, 115.21, 77.33, 77.02, 76.70, 68.04, 48.03, 37.48, 31.99, 29.73, 29.67, 29.47, 29.43, 29.14, 26.04, 22.75, 14.16. MALDI-TOF MS: [M+Na]⁺ calculated for $\text{C}_{86}\text{H}_{82}\text{O}_2\text{Na}$: 1170.5598; found, 1170.5622. m.p.: 208.2 °C.

The molecule (TBFC12) 1,4-bis(17H-tetrabenzo[a,c,g,i]fluorenemethyl)-2,5-bis(dodecyloxy)benzene: ^1H NMR (400 MHz, CDCl_3): δ 8.78 (d, $J = 8$ Hz, 4H), 8.73 (d, $J = 8$ Hz, 4H), 8.60 (d, $J = 8$ Hz, 4H), 7.92 (d, $J = 8.1$ Hz, 4H), 7.66-7.73 (m, 4H), 7.51-7.63 (m, 8H), 7.36-7.43 (m, 4H), 5.38 (s, 2H), 5.16 (t, $J = 6$ Hz, 2H), 3.25 (d, $J = 6$ Hz, 4H), 2.61 (t, $J = 7$ Hz, 4H), 1.12-1.40 (m, 40H), 0.90 (t, $J = 7$ Hz, 6H). ^{13}C NMR (101 MHz, CDCl_3) δ 150.37, 145.68, 135.83, 131.30, 130.11, 129.14, 128.36, 127.47, 126.12, 125.87, 125.59, 125.54, 125.01, 124.90, 123.45, 122.87, 115.21, 77.33, 77.02, 76.70, 68.04, 48.03, 37.49,

31.98, 29.79, 29.73, 29.47, 29.43, 29.14, 26.04, 22.74, 14.15. MALDI-TOF MS: [M+Na]⁺ calculated for C₉₀H₉₀O₂Na: 1225.6839; found, 1225.6844. m.p.: 202.3 °C.

The molecule (TBFC14) 1,4-bis(17H-tetrabenzo[a,c,g,i]fluorenemethyl)-2,5-bis(tetradecyloxy)benzene: ¹H NMR (400 MHz, CDCl₃) δ 8.78 (d, J = 8.2 Hz, 4H), 8.68 (t, J = 23.2 Hz, 4H), 8.59 (d, J = 8.2 Hz, 4H), 7.91 (d, J = 8.0 Hz, 4H), 7.65-7.73 (m, 4H), 7.61 – 7.47 (m, 8H), 7.34-7.44 (m, 4H), 5.34 (d, J= 32.2 Hz, 2H), 5.16 (t, J = 6.1 Hz, 2H), 3.24 (d, J = 5.7 Hz, 4H), 2.60 (t, J = 6.7 Hz, 4H), 1.40 – 1.04 (m, 48H), 0.89 (t, J = 6.7 Hz, 6H). ¹³C NMR (101 MHz, CDCl₃) δ 150.37, 145.69, 135.83, 131.30, 130.11, 129.13, 128.36, 127.47, 126.12, 125.87, 125.59, 125.54, 125.01, 124.90, 123.45, 122.87, 115.21, 77.33, 77.02, 76.70, 68.04, 48.03, 31.96, 29.79, 29.72, 29.46, 29.41, 29.14, 26.04, 22.72, 14.14. MALDI-TOF MS: [M+Na]⁺ calculated for C₉₄H₉₈O₂Na: 1281.7465; found, 1281.771. m.p.: 181.8 °C.

The molecule (TBFC18) 1,4-bis(17H-tetrabenzo[a,c,g,i]fluorenemethyl)-2,5-bis(octyldecyloxy)benzene: ¹H NMR (400 MHz, CDCl₃) δ 8.76 (d, J = 8.0 Hz, 4H), 8.70 (d, J = 8.3 Hz, 4H), 8.58 (d, J = 8.0 Hz, 4H), 7.94 (d, J = 8.1 Hz, 4H), 7.59 – 7.71 (m, 4H), 7.44 – 7.59 (m, 8H), 7.34-7.45 (m, 4H), 5.32 (s, 2H),, 5.14 (t, J = 6.1 Hz, 2H), 3.30 (d, J = 5.8 Hz, 4H), 2.59 (t, J = 6.8 Hz, 4H), 1.46 – 0.93 (m, 64H), 0.87 (t, J = 6.8 Hz, 6H). ¹³C NMR (101 MHz, CDCl₃) δ 150.37, 145.69, 135.84, 131.30, 130.11, 129.14, 128.37, 127.47, 126.12, 125.88, 125.59, 125.54, 125.02, 124.90, 123.45, 122.87, 115.22, 77.35, 77.03, 76.71, 68.04, 48.03, 37.50, 31.96, 29.81, 29.76, 29.74, 29.71, 29.48, 29.40, 29.15, 26.05, 22.72, 14.14. MALDI-TOF MS: [M+Na]⁺ calculated for C₁₀₂H₁₁₄O₂Na: 1393.8717; found, 1393.2012. m.p.: 167.6 °C.

Section B: TGA spectra of TBFC8 to TBFC18

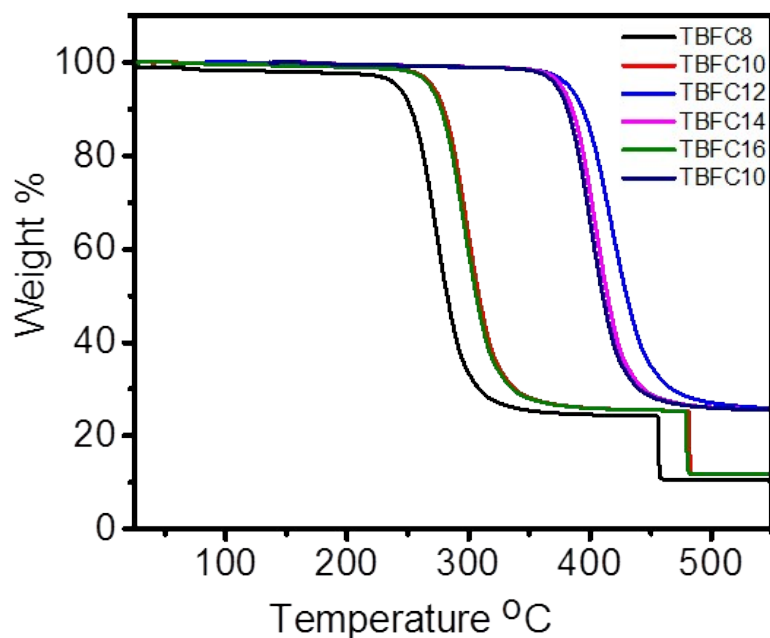


Figure S13. TGA curves of TBFC8 to TBFC18 at heating rate of 10 °C/min under N₂ atmosphere.

Molecule name	TBFC8	TBFC10	TBFC12	TBFC14	TBF16	TBFC18
Decomposition temperature °C at 95%	241.3 °C	270.4 °C	382.3 °C	376.2 °C	268.1 °C	372.2 °C

Section C: DSC spectra and HOPM images of TBFC8 to TBFC18

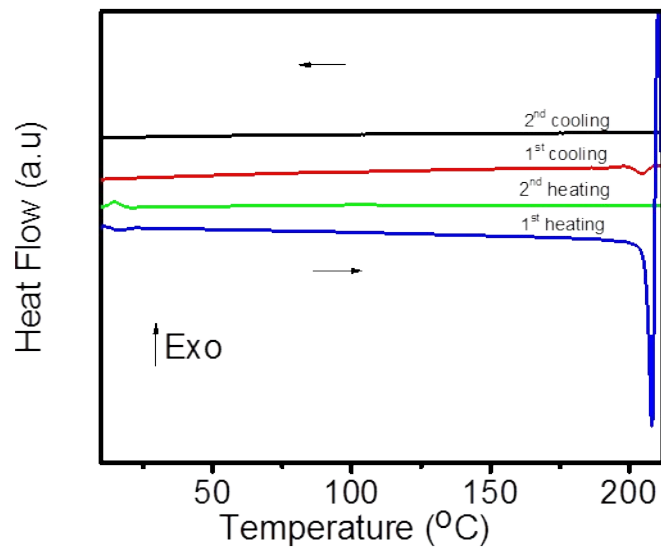


Figure S14. DSC trace of TBFC8 at 20 °C/min first cycle and 5 °C/min second cycle under N₂ atmosphere.

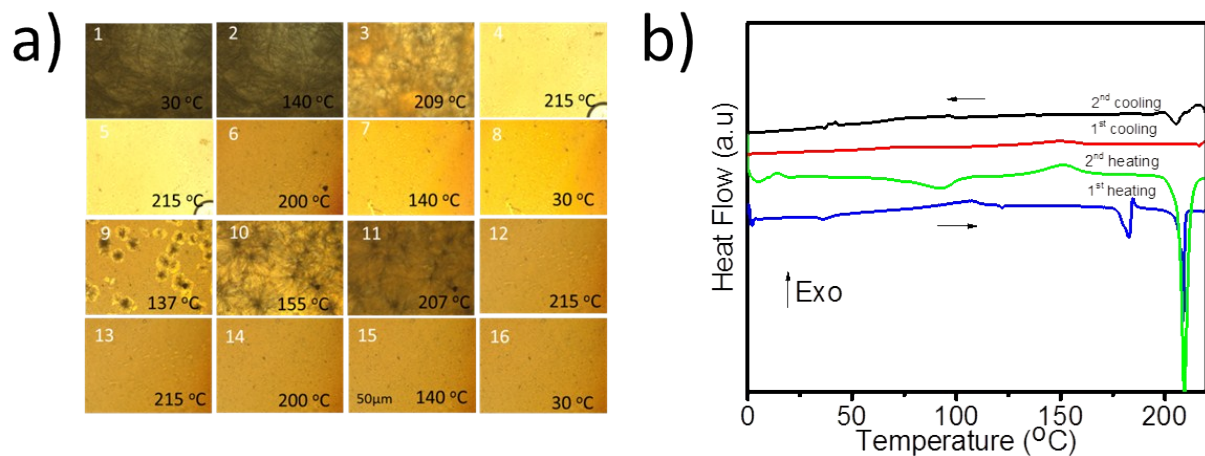


Figure S15. **a)** HOPM images of TBFC10 with two heating and cooling cycle (First and second rows corresponds to first heating and cooling cycle, third and fourth rows corresponds to second heating and cooling cycle). **b)** DSC trace of TBFC10 at 20 °C/min first cycle and 5 °C/min second cycle under N₂ atmosphere.

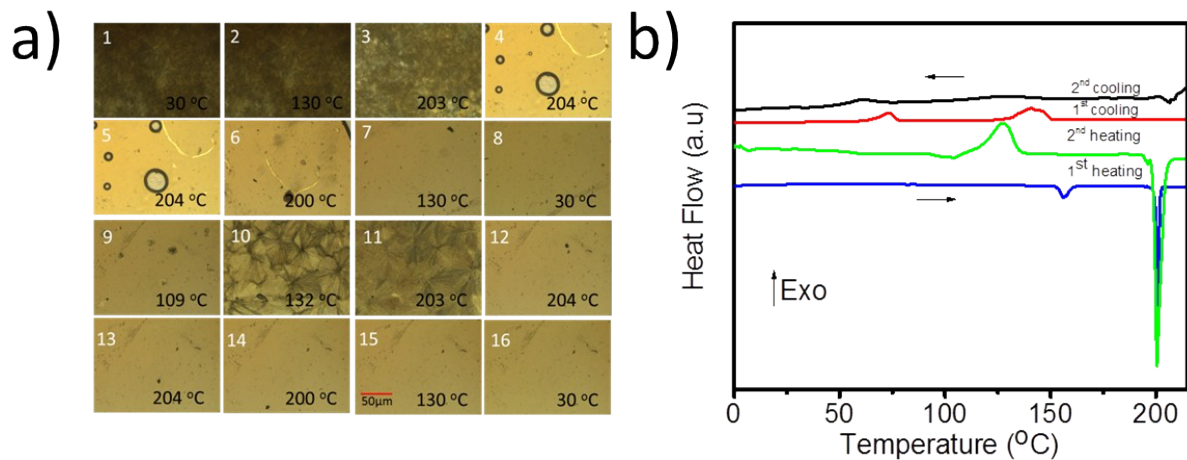


Figure S16. **a)** HOPM images of TBFC12 with two heating and cooling cycle (First and second rows corresponds to first heating and third and fourth rows corresponds to second heating and cooling cycle). **b)** DSC trace of TBFC12 at 20 °C/min first cycle and 5 °C/min second cycle under N₂ atmosphere.

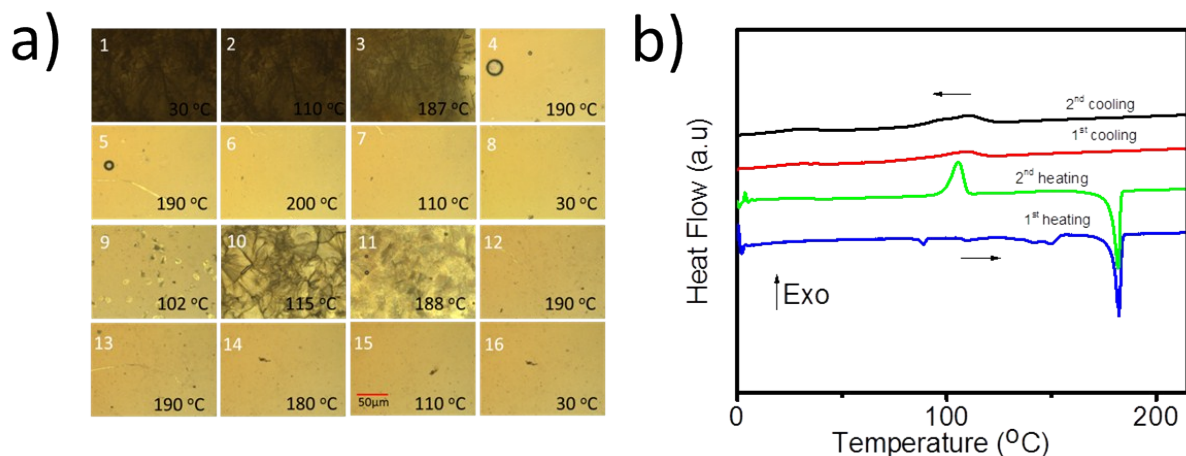


Figure S17. **a)** HOPM images of TBFC14 with two heating and cooling cycle (First and second rows corresponds to first heating and cooling cycle, third and fourth rows corresponds to second heating and cooling cycle). **b)** DSC trace of TBFC14 at 20 °C/min first cycle and 5 °C/min second cycle under N₂ atmosphere.

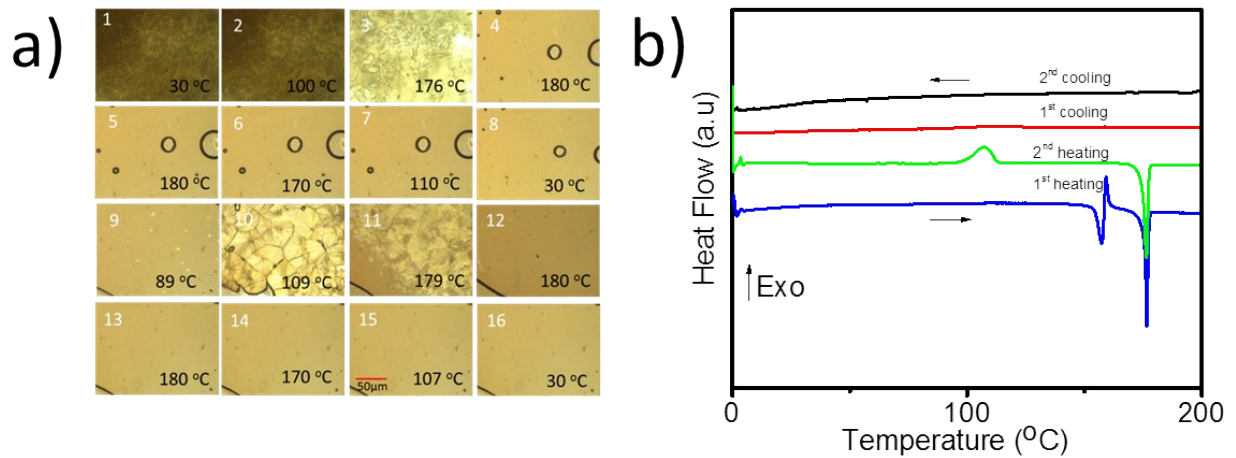


Figure S18. **a)** HOPM images of TBFC16 with two heating and cooling cycle (First and second rows corresponds to first heating and cooling cycle, third and fourth rows corresponds to second heating and cooling cycle). **b)** DSC trace of TBFC16 at 20 °C/min first cycle and 5 °C/min second cycle under N₂ atmosphere.

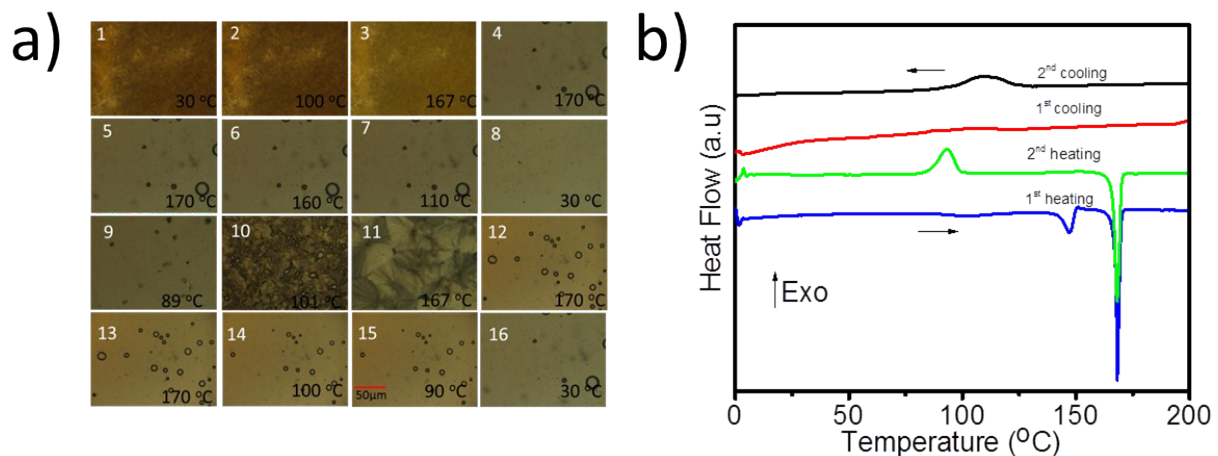


Figure S19. **a)** HOPM images of TBFC18 with two heating and cooling cycle (First and second rows corresponds to first heating and cooling cycle, third and fourth rows corresponds to second heating and cooling cycle). **b)** DSC trace of TBFC18 at 20 °C/min first cycle and 5 °C/min second cycle under N₂ atmosphere.

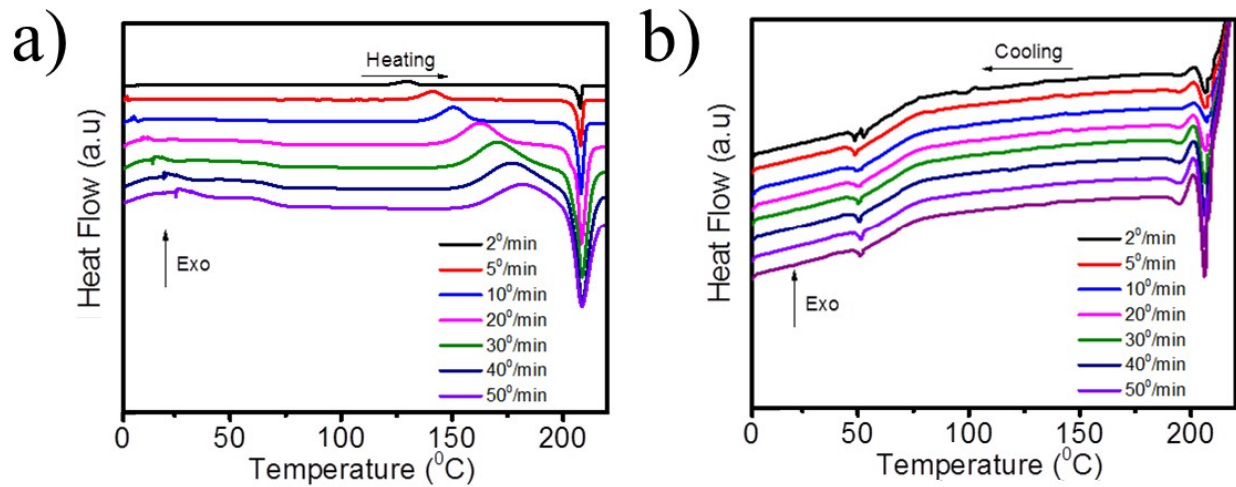


Figure S20. **a)** Heating traces of TBFC10 with varying heating rates while the cooling rate is kept constant at 10 $^{\circ}\text{C}/\text{min}$. **b)** Cooling traces of TBFC10 with varying cooling rates and constant heating rate at 10 $^{\circ}\text{C}/\text{min}$.

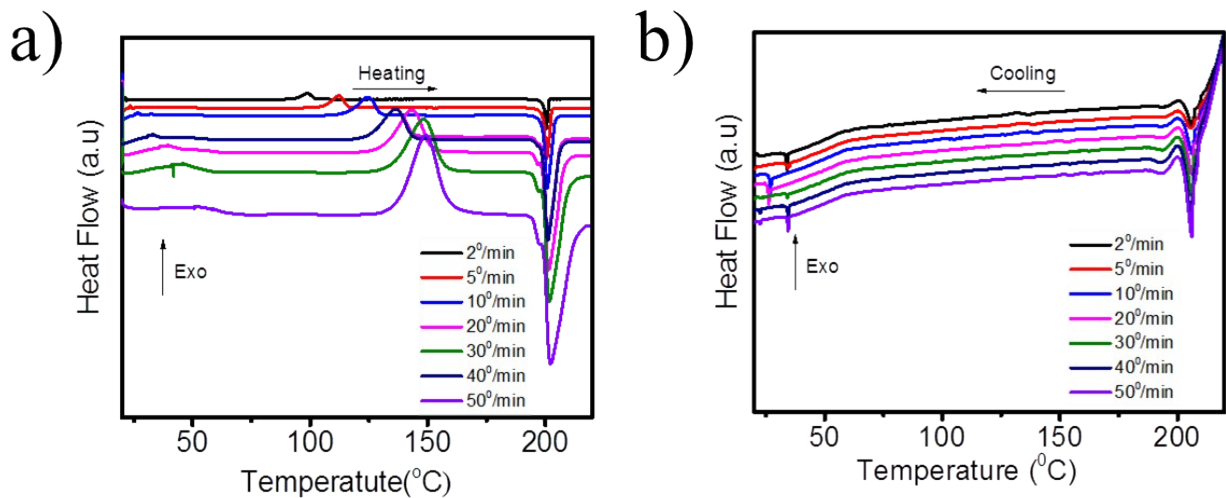


Figure S21. **a)** Heating traces of TBFC12 with varying heating rates while the cooling rate is kept constant at 10 $^{\circ}\text{C}/\text{min}$. **b)** Cooling traces of TBFC12 with varying cooling rates and constant heating rate at 10 $^{\circ}\text{C}/\text{min}$.

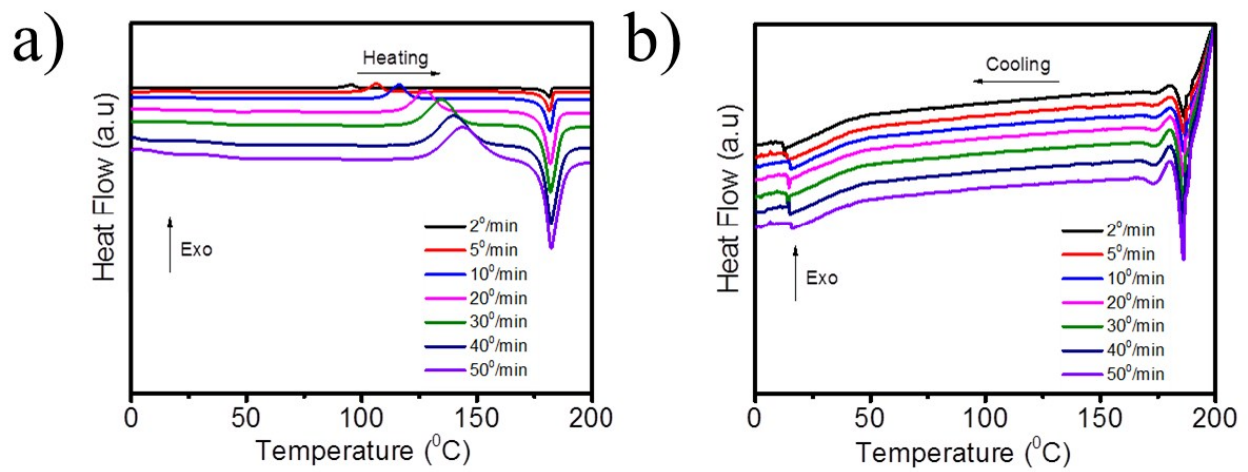


Figure S22. **a)** Heating traces of TBFC14 with varying heating rates while the cooling rate is kept constant at 10 °C/min. **b)** Cooling traces of TBFC14 with varying cooling rates and constant heating rate at 10 °C/min.

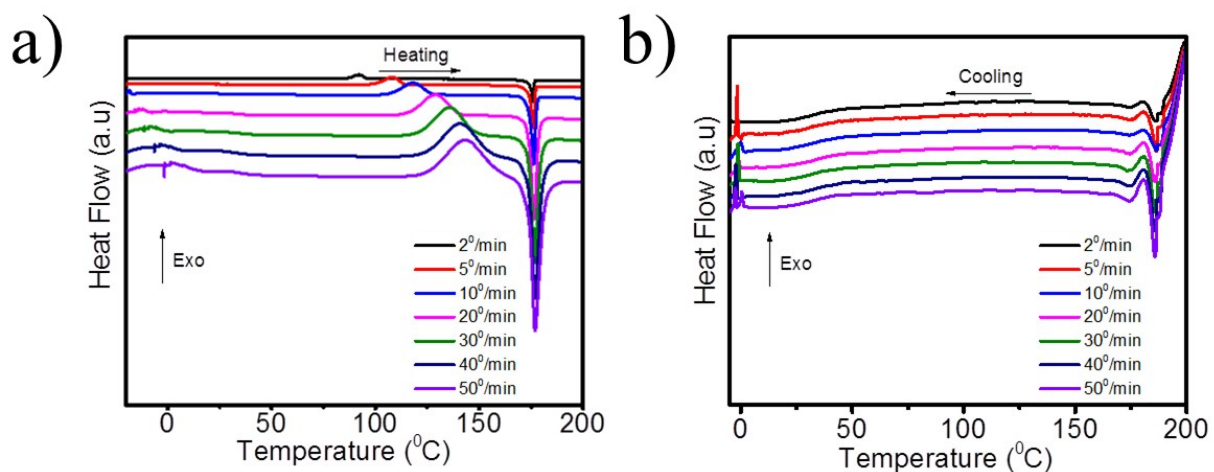


Figure S23. **a)** Heating traces of TBFC16 with varying heating rates while the cooling rate is kept constant at 10 °C/min. **b)** Cooling traces of TBFC16 with varying cooling rates and constant heating rate at 10 °C/min.

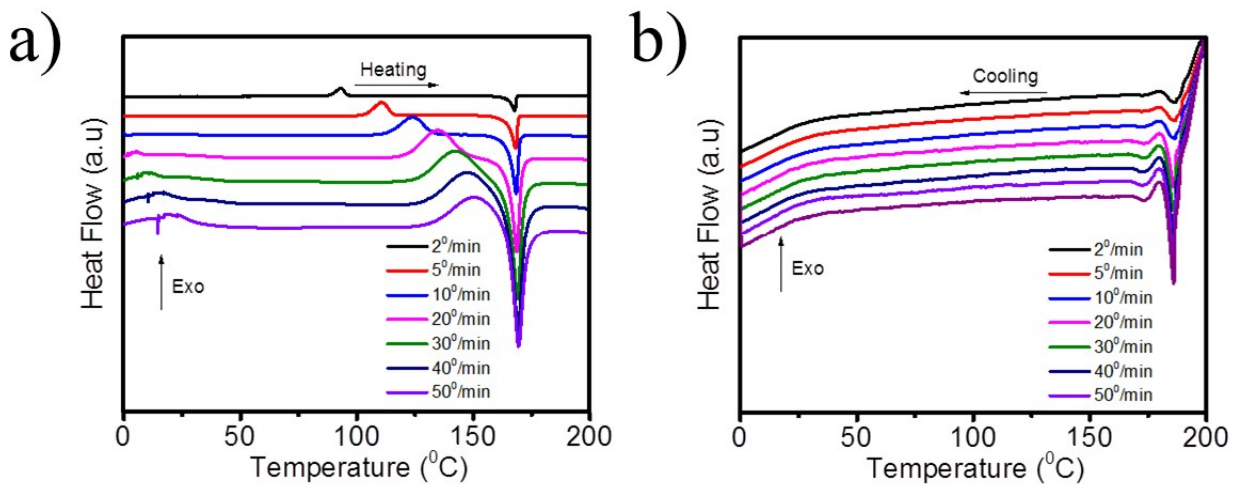


Figure S24. **a)** Heating traces of TBFC18 with varying heating rates while the cooling rate is kept constant at 10 °C/min. **b)** Cooling traces of TBFC18 with varying cooling rates and constant heating rate at 10 °C/min.

Table S1. DSC spectra details of TBFC10 as a function of heating rate

S. No	λ (K/min)	T_p (K)	ΔH_{cc} (kJ/mol)	T_m (°C)	ΔH_m (kJ/mol)
1	2	402.7	24.66	207.7	-39.18
2	5	414.5	27.28	207.8	-38.83
3	10	423.6	29.11	208.0	-37.74
4	20	435.3	27.6	208.3	-35.68
5	30	443.3	25.76	208.5	-34.52
6	40	450.1	16.73	208.7	-32.78
7	50	454.9	7.73	208.8	-23.61

Table S2. DSC spectra details of TBFC12 as a function of heating rate

S. No	λ (K/min)	T_p (K)	ΔH_{cc} (kJ/mol)	T_m (°C)	ΔH_m (kJ/mol)
1	2	371.8	29.7	200.5	-49.38
2	5	385.2	28.37	200.7	-49.64
3	10	397.8	32.75	200.8	-49.44
4	20	409.3	35.38	201.1	-48.84
5	30	416.3	36.89	201.4	-41.85
6	40	421.2	36.28	201.7	-38.58
7	50	425.4	36.64	202.0	-37.8

Table S3. DSC spectra details of TBFC14 as a function of heating rate

S. No	λ (K/min)	T_p (K)	ΔH_{cc} (kJ/mol)	T_m (°C)	ΔH_m (kJ/mol)
1	2	368.5	28	181.4	-35.75
2	5	379.4	30.01	181.6	-39.59
3	10	389.3	33.48	181.7	-39.93
4	20	400.4	33.18	181.8	-39.44
5	30	407.6	33.51	182	-39.21
6	40	412.9	33.60	182.1	-39.55
7	50	416.9	33.73	182.3	-40.05

Table S4. DSC spectra details of TBFC18 as a function of heating rate

S. No	λ (K/min)	T_p (K)	ΔH_{cc} (kJ/mol)	T_m (°C)	ΔH_m (kJ/mol)
1	2	365.2	31.12	176	-50.83
2	5	381.5	33.72	176.2	-48.72
3	10	390.9	35.72	176.3	-47.21
4	20	401.6	37.56	176.4	-46.14
5	30	409.1	39.36	176.6	-45.36
6	40	413.7	39.79	176.8	-45.32
7	50	416.4	40.66	177.0	-45.02

Section D: Kissinger activation energy plot¹ of molecule TBFC10, TBFC12, TBFC14 and TBFC18

Kissinger equation:

$$\ln(\lambda/T_p^2) = -E_a/RT_p + C \quad (1)$$

Where R is gas constant, T_p is crystallization peak temperature, λ is DSC heating rate, E_a is the crystallization activation energy and C is a constant¹. The slope of $\ln(\lambda/T_p^2)$ vs $1/T_p$ gives the value for E_a/R .

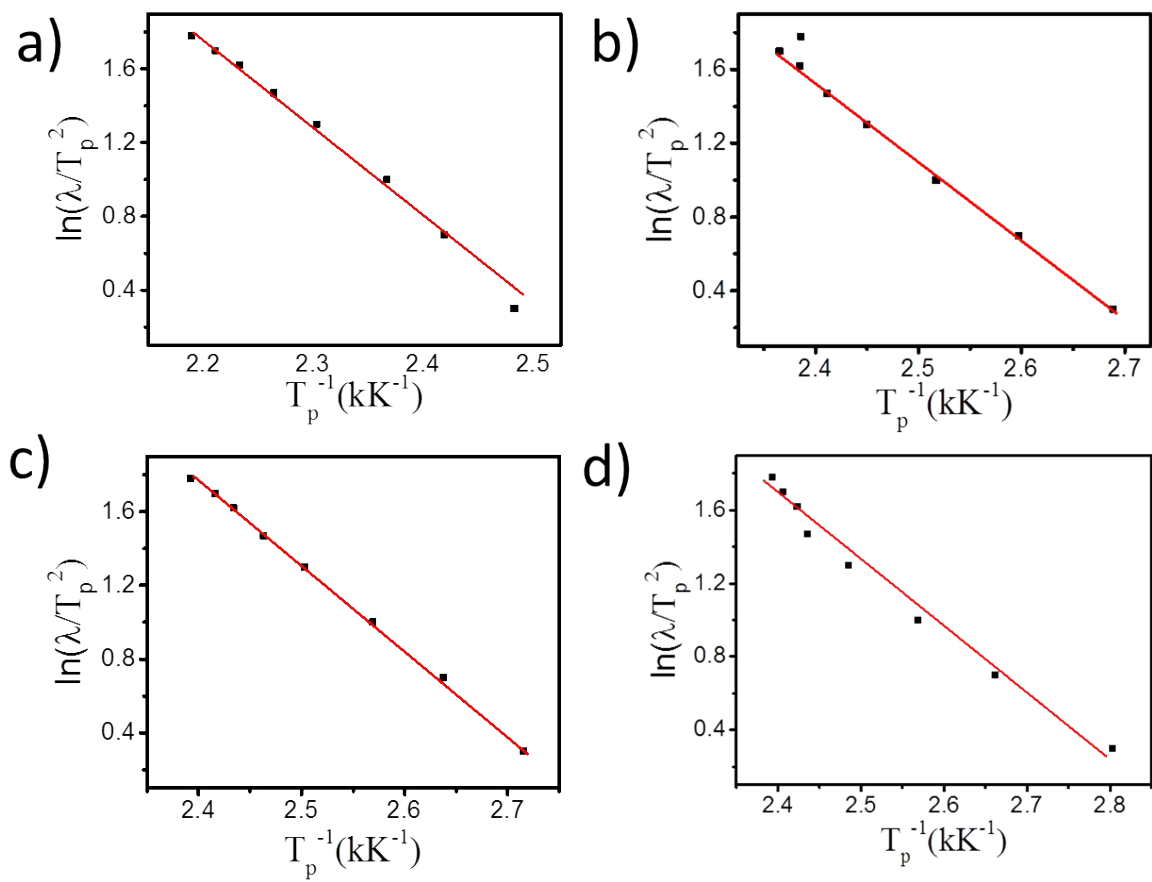


Figure S25. Kissinger activaiton energy (E_a) plot of molecule TBFC10, TBFC12, TBFC14 and TBFC18. **a)** TBFC10 E_a Plot and E_a is $90.35 \pm 3.10 \text{ kJ/mol}$ **b)** TBFC12 E_a Plot and E_a is $79.10 \pm 4.04 \text{ kJ/mol}$ **c)** TBFC14 E_a Plot and E_a is $81.250 \pm 1.00 \text{ kJ/mol}$ and **d)** TBFC18 E_a Plot and E_a is $62.18 \pm 3.16 \text{ kJ/mol}$.

Section E: Relative crystallinity verses temperature plot² of molecule TBFC10 and TBFC12.

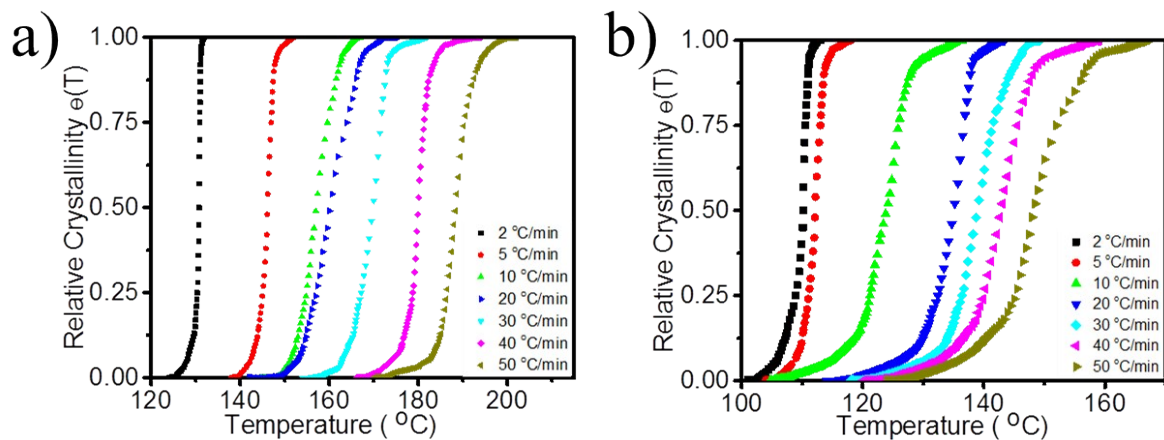


Figure S26. Relative crystallinity $\Theta(T)$ versus temerature for TBFC10 and TBFC12 at seven different heating rates. These curves have been converted from **Figure S20** and **Figure S21** and using Avrami equation 3².

Section F: Ozawa-Flynn-Wall activation energy plot³ of molecule TBFC10 and TBFC18

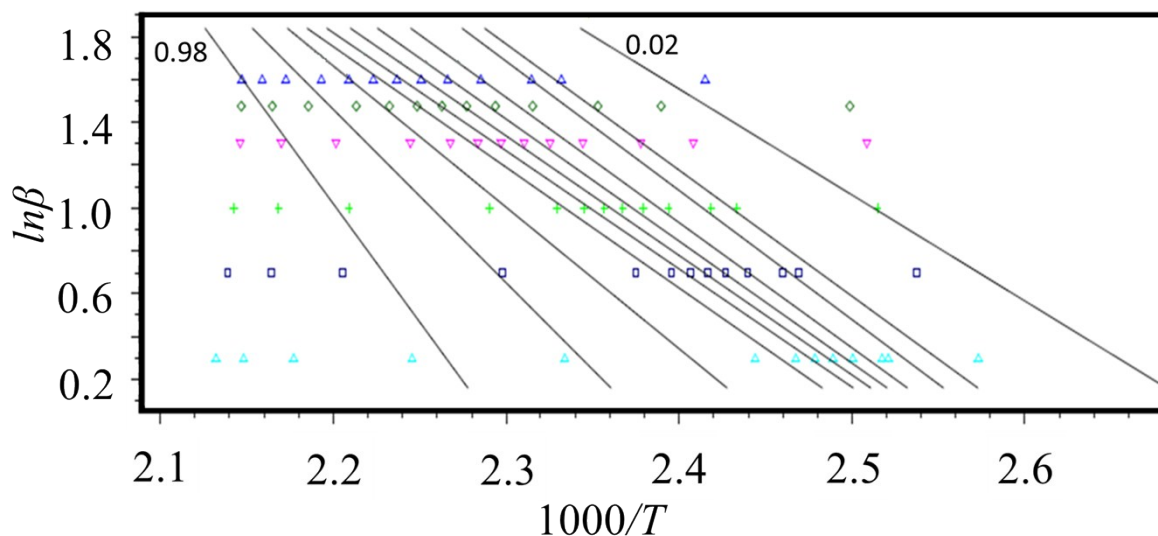


Figure S27. Ozawa-Flynn-Wall analysis activation energy plot of molecule TBFC10 and E_a is 90.35 ± 3.10 kJ/mol.

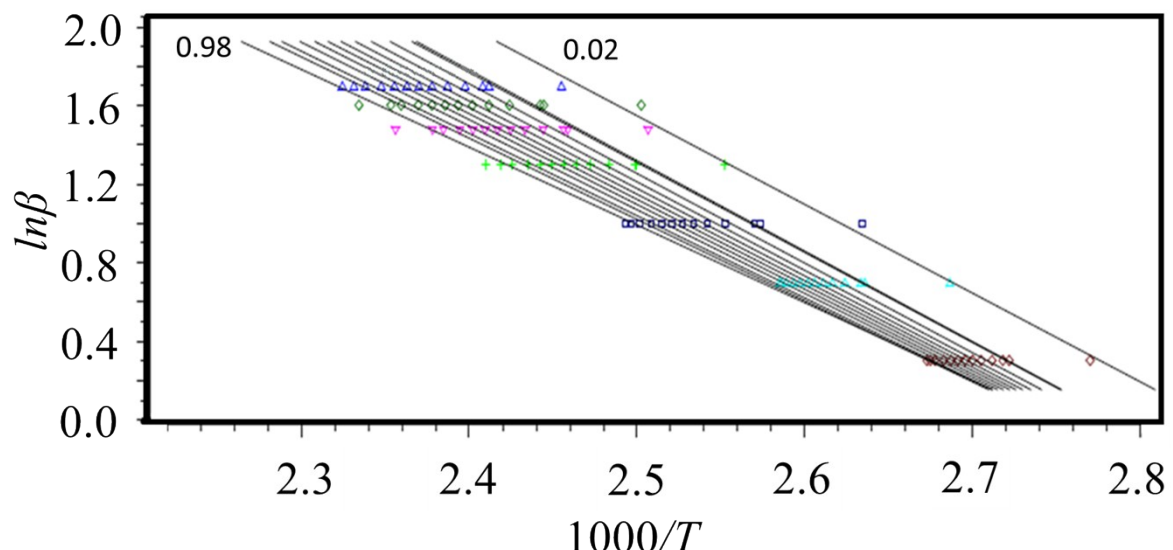


Figure S28. Ozawa-Flynn-Wall analysis activation energy plot of molecule TBFC12 and E_a is 79.10 ± 4.04 kJ/mol.

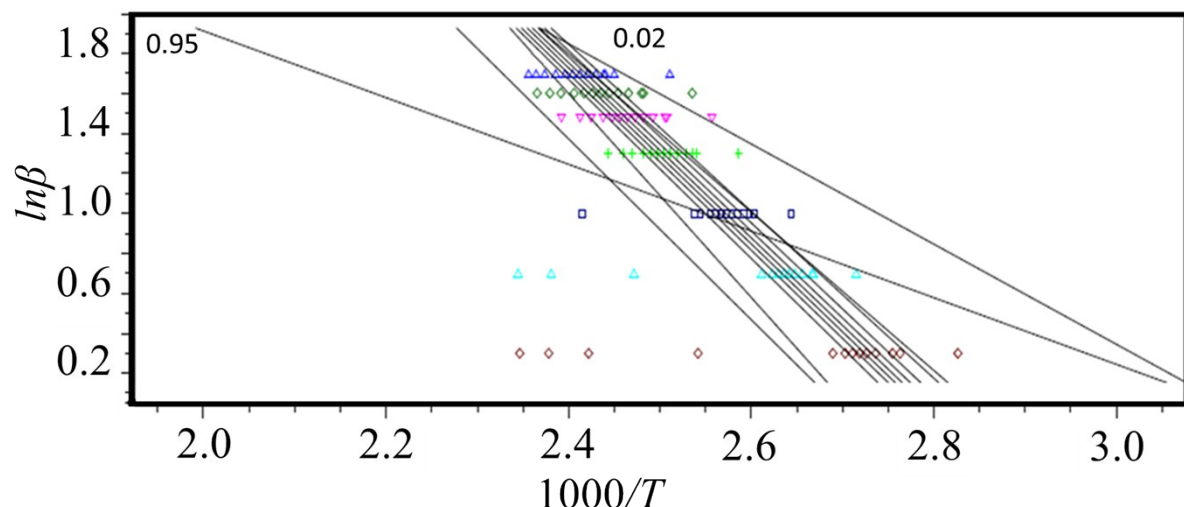


Figure S29 . Ozawa-Flynn-Wall analysis activation energy plot of molecule TBFC14 and E_a is 81.25 ± 1.00 kJ/mol.

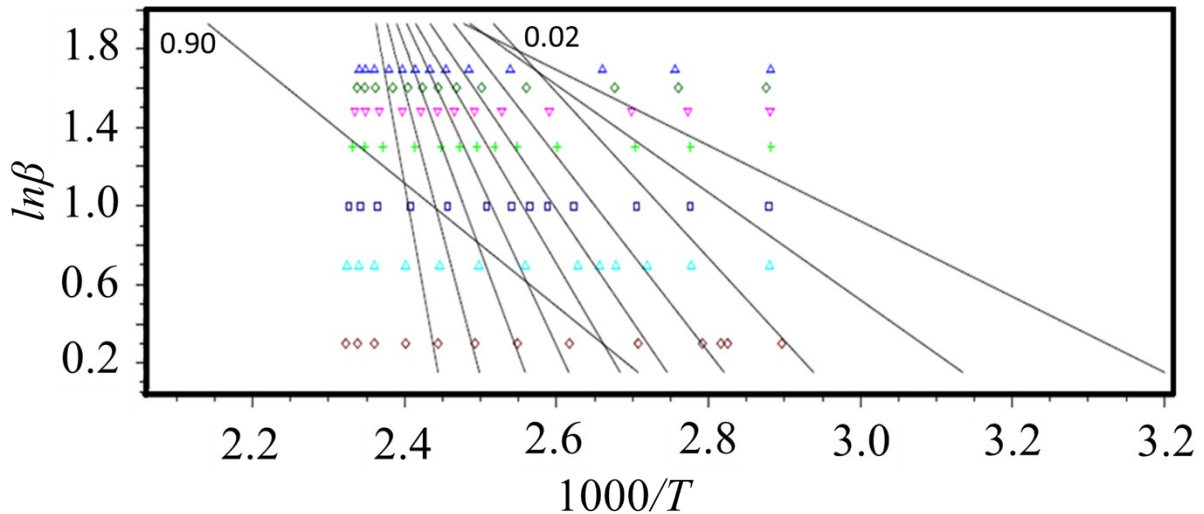


Figure S30. Ozawa-Flynn-Wall analysis activation energy plot of molecule TBFC18 and E_a is 62.18 ± 3.16 kJ/mol.

Table S5. The conversion percentage of α values of TBF10 to TBF18.

conversion percentage (α)	Activation Energy (kJ/mol)				
	TBFC10	TBFC12	TBFC14	TBFC16	TBFC18
0.02	88.40 ± 27.34	80.43 ± 2.73	42.45 ± 24.71	80.10 ± 4.91	31.81 ± 25.60
0.05	105.85 ± 16.21	81.55 ± 1.70	69.68 ± 5.68	82.17 ± 2.99	46.90 ± 27.81
0.1	108.58 ± 8.37	81.99 ± 1.75	73.77 ± 5.52	85.33 ± 2.88	74.64 ± 25.33
0.2	105.58 ± 4.28	81.15 ± 2.38	76.25 ± 4.77	85.32 ± 3.10	89.21 ± 11.28
0.3	102.24 ± 3.04	80.07 ± 2.78	77.16 ± 4.17	84.65 ± 3.27	102.61 ± 6.59
0.4	99.95 ± 2.61	79.07 ± 3.03	77.61 ± 3.66	84.05 ± 3.34	119.60 ± 14.02
0.5	98.58 ± 2.64	78.14 ± 3.20	77.91 ± 3.24	83.91 ± 3.29	152.95 ± 25.24
0.6	100.93 ± 4.20	77.25 ± 3.33	78.29 ± 2.94	91.29 ± 3.39	194.04 ± 46.72
0.7	119.22 ± 26.35	76.33 ± 3.42	79.48 ± 3.02	106.77 ± 14.65	273.92 ± 46.72
0.8	147.77 ± 64.35	75.30 ± 3.50	91.28 ± 19.82	104.71 ± 27.66	410.0 ± 201.53
0.9	203.85 ± 224.56	73.89 ± 3.58	80.22 ± 51.52	121.10 ± 53.44	53.65 ± 784.22
0.95	-342.30 ± 532.55	72.88 ± 3.64	26.42 ± 53.40	115.95 ± 86.33	

0.98	-1649.93 ± 179.4	69.49 ± 4.03		66.43 ± 175.19	
------	----------------------	------------------	--	--------------------	--

Section G: Isothermal crystallization with five different temperatures range.

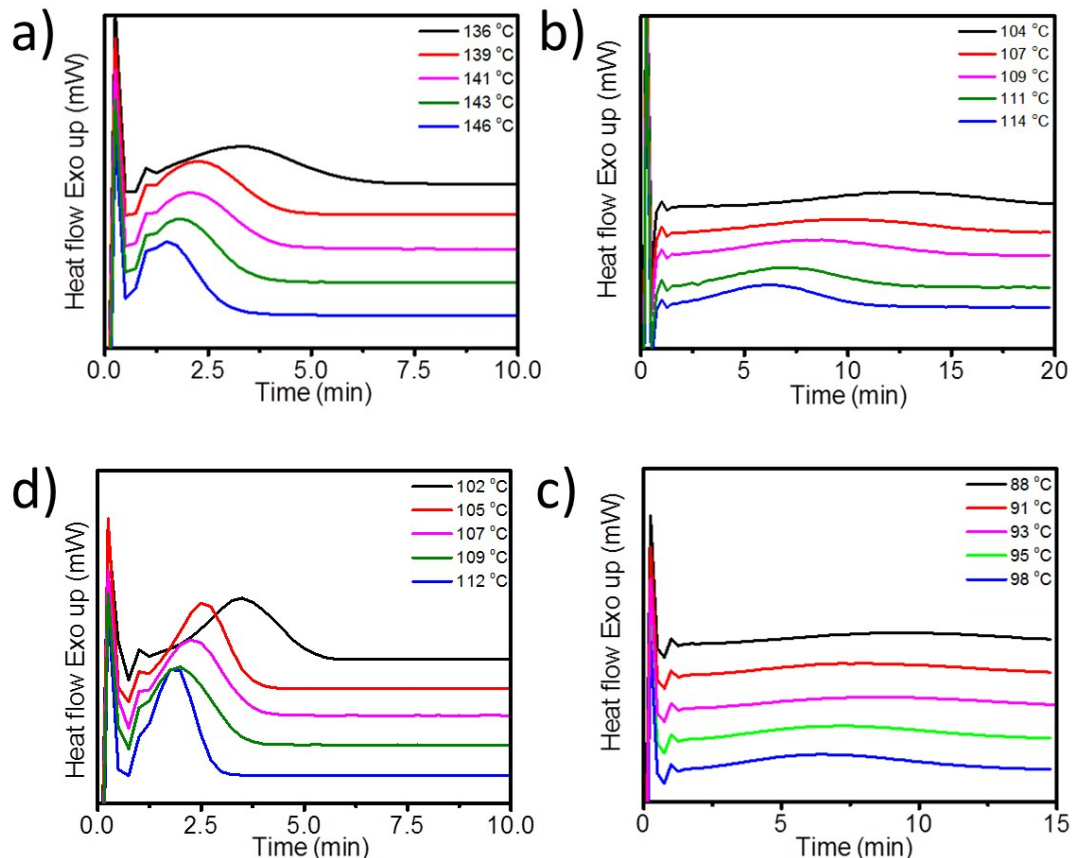


Figure S31. Isothermal crystallization of TBFC10, TBFC12, TBFC14 and TBFC18 with five different temperature range. a) Isothermal crystallization plot of TBFC10. b) Isothermal crystallization plot of TBFC12. c) Isothermal crystallization plot of TBFC14 and d) Isothermal crystallization plot of TBFC18.

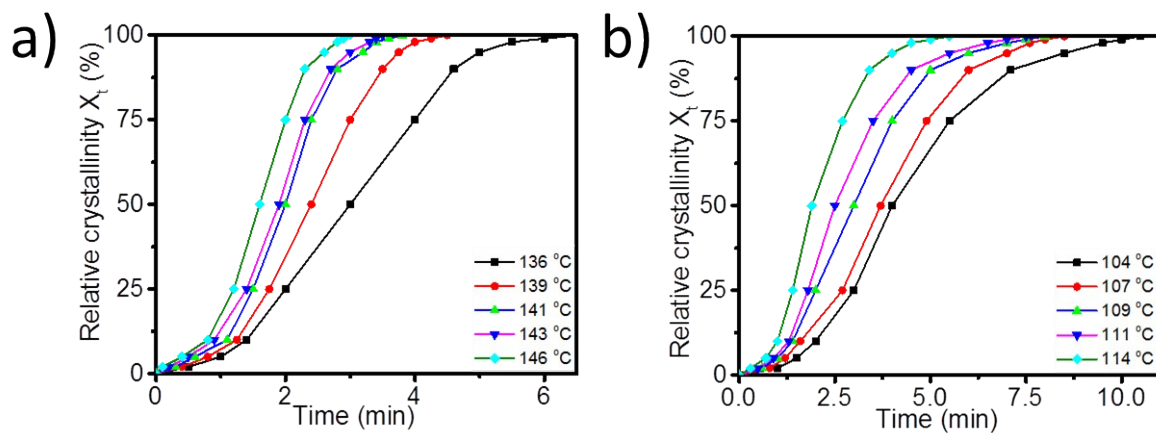


Figure S32. Relative crystallinity⁴ with crystallization time during isothermal crystallization of molecule TBFC10 (**Figure a)** and **b** respect to molecule TBFC12 at five different temperatures range.

Section H: PXRD 2θ peaks intensity, FWHM (deg) and crystal size values.

Table S6. 2θ peaks intensity, FWHM (deg) and crystal size values of TBFC8.

2-theta (deg)	d (ang.)	Height (cps)	Int. I(cps deg)	FWHM(deg)	Size
5.473(4)	16.134(10)	4374(242)	1802(21)	0.318(4)	261(4)
10.308(15)	8.574(12)	272(60)	154(5)	0.34(2)	245(17)
12.197(13)	7.251(7)	301(63)	98(7)	0.259(14)	323(18)
12.773(13)	6.925(7)	213(53)	98(7)	0.36(4)	229(22)
16.68(3)	5.310(8)	208(53)	161(6)	0.41(4)	202(18)
19.64(2)	4.517(5)	207(52)	163(9)	0.38(4)	223(24)
20.145(12)	4.404(3)	172(48)	34(7)	0.09(3)	890(239)
22.28(5)	3.986(9)	101(37)	125(8)	0.80(7)	106(9)
23.79(2)	3.737(4)	259(59)	94(5)	0.26(3)	324(32)
24.399(17)	3.645(2)	255(58)	112(5)	0.27(3)	316(32)

Table S7. 2θ peaks intensity, FWHM (deg) and crystal size values of TBFC10.

2-theta (deg)	d (ang.)	Height (cps)	Int. I(cps deg)	FWHM(deg)	Size
5.72(4)	15.44(12)	1006(116)	1031(1090)	0.81(14)	102(18)
6.88(2)	12.83(4)	416(74)	197(9)	0.44(2)	187(10)
7.731(13)	11.43(2)	984(115)	449(16)	0.429(12)	194(5)
9.095(13)	9.715(14)	362(69)	138(5)	0.359(10)	232(7)
10.146(12)	8.711(10)	399(73)	163(4)	0.384(9)	217(5)
11.96(2)	7.395(13)	134(42)	69(3)	0.45(2)	184(10)
13.78(2)	6.420(11)	358(69)	190(8)	0.47(2)	180(8)
18.64(12)	4.76(3)	64(29)	158(11)	2.2(3)	38(4)
20.56(2)	4.316(5)	477(80)	316(8)	0.48(2)	174(8)
27.6(5)	3.23(6)	17(15)	32(12)	1.3(6)	65(30)

Table S8. 2θ peaks intensity, FWHM (deg) and crystal size values of TBFC12.

2-theta (deg)	d (ang.)	Height (cps)	Int. I(cps deg)	FWHM(deg)	Size
4.658(2)	18.954(9)	18466(496)	5428(29)	0.2395(18)	347(3)
9.465(5)	9.336(5)	1721(151)	596(7)	0.303(4)	275(4)
10.24(3)	8.64(2)	116(39)	40(3)	0.30(2)	274(21)
11.80(6)	7.49(4)	63(29)	35(4)	0.44(6)	189(27)
13.238(16)	6.683(8)	249(58)	82(4)	0.310(12)	269(11)
14.42(3)	6.136(13)	82(33)	24(2)	0.27(3)	306(30)
16.870(15)	5.251(5)	421(75)	266(7)	0.531(14)	158(4)
19.351(7)	4.5832(16)	1441(139)	473(7)	0.275(6)	306(6)
21.101(13)	4.207(3)	334(67)	101(4)	0.263(12)	321(15)
21.66(3)	4.100(6)	117(39)	29(3)	0.21(3)	396(53)

23.78(3)	3.738(5)	162(46)	40(4)	0.22(3)	392(55)
----------	----------	---------	-------	---------	---------

Table S9. 2θ peaks intensity, FWHM (deg) and crystal size values of TBFC14.

2-theta (deg)	d (ang.)	Height (cps)	Int. I(cps deg)	FWHM(deg)	Size
4.098(5)	21.54(3)	1596(146)	735(11)	0.313(8)	266(7)
4.530(8)	19.49(3)	662(94)	251(9)	0.262(13)	317(16)
5.70(2)	15.48(6)	393(72)	126(8)	0.21(3)	395(54)
8.18(8)	10.80(11)	94(35)	23(10)	0.23(8)	357(124)
13.44(6)	6.58(3)	62(29)	23(4)	0.31(7)	272(62)
14.22(3)	6.225(13)	105(37)	32(4)	0.27(3)	314(37)
20.36(4)	4.359(8)	215(54)	179(13)	0.52(6)	161(18)
21.47(7)	4.136(14)	126(41)	156(15)	0.76(12)	111(17)
23.52(7)	3.779(10)	151(45)	242(18)	1.09(8)	78(6)
27.6(6)	3.23(7)	23(18)	224(28)	6.3(10)	14(2)

Table S10. 2θ peaks intensity, FWHM (deg) and crystal size values of TBFC16.

2-theta (deg)	d (ang.)	Height (cps)	Int. I(cps deg)	FWHM(deg)	Size
3.755(5)	23.51(3)	2119(168)	954(10)	0.287(8)	289(8)
6.370(4)	13.863(9)	2307(175)	1071(9)	0.374(4)	222(2)
7.327(17)	12.06(3)	231(56)	134(4)	0.476(19)	175(7)
10.241(14)	8.630(11)	253(58)	108(4)	0.394(13)	211(7)
11.51(3)	7.684(18)	116(39)	50(2)	0.40(2)	207(11)
14.70(2)	6.021(9)	230(55)	217(7)	0.79(3)	107(4)

17.452(19)	5.077(6)	308(64)	244(7)	0.56(2)	150(7)
19.658(19)	4.512(4)	369(70)	300(9)	0.63(2)	133(5)
20.711(13)	4.285(3)	574(87)	357(11)	0.478(17)	176(6)
22.42(3)	3.963(5)	195(51)	121(6)	0.54(3)	156(8)
25.38(8)	3.506(11)	64(29)	81(10)	1.10(12)	78(9)

Table S11. 2θ peaks intensity, FWHM (deg) and crystal size values of TBFC18.

2-theta (deg)	d (ang.)	Height (cps)	Int. I (cps deg)	FWHM(deg)	Size
3.634(6)	24.29(4)	3075(202)	1544(19)	0.320(9)	260(7)
6.171(4)	14.310(9)	2381(178)	1133(10)	0.400(4)	207(2)
7.607(18)	11.61(3)	222(54)	139(5)	0.53(2)	158(6)
8.262(14)	10.693(19)	232(56)	109(5)	0.40(2)	210(13)
10.311(15)	8.572(13)	363(70)	172(5)	0.379(14)	220(8)
11.81(5)	7.49(3)	89(34)	53(4)	0.55(4)	153(12)
14.361(16)	6.163(7)	346(68)	225(7)	0.516(17)	162(5)
15.291(10)	5.790(4)	342(67)	147(6)	0.363(17)	231(11)
19.856(16)	4.468(4)	553(86)	462(28)	0.66(3)	128(5)
20.774(12)	4.272(3)	774(102)	688(28)	0.64(3)	132(6)
25.71(3)	3.462(5)	165(47)	90(6)	0.51(3)	167(10)

Section I: Table S12 2θ and h, k, l values of TBFC12 form single crystal PXRD .

2 theta values	4.933	8.997	10.448	10.650	12.164	13.576	15.720	17.511	18.217
h, k, l values	0,0,1	0,1,0	0,1,1	1,1,0	1,1,-1	0,1,-2	1,-1,0	0,1,-3	1,0,-3
2 theta values	18.621	20.336	20.946	21.648	22.354	22.758	24.271	24.675	25.179
h, k, l values	1,-1,-2	1,2,-2	0,2,-2	1,2,3	2,2,-1	2,0,-2	2,2,-2	2,1,-3	1,3,0

Section J: References

1. H. E. Kissinger, *J. Res. Natl. Bur. Stand*, 1956, **57**, 217-221.
2. T. Liu, Z. Mo, S. Wang and H. Zhang, *Polym. Eng. Sci*, 1997, **37**, 568-575.
3. O. Bianchi, R. Oliveira, R. Fiorio, J. D. N. Martins, A. Zattera and L. Canto, *Polym. Test*, 2008, **27**, 722-729.
4. X. Lu and J. Hay, *Polymer*, 2001, **42**, 9423-9431.